Cu₂Mo₆S₈ Chevrel Phase, A Promising Cathode Material for New Rechargeable Mg Batteries: A Mechanically Induced Chemical Reaction

Elena Levi, Yossi Gofer, Yulia Vestfreed, Eli Lancry, and Doron Aurbach*

Department of Chemistry, Bar-Ilan University, Ramat-Gan, Israel 52900

Received January 21, 2002. Revised Manuscript Received March 14, 2002

This paper deals with the correlation between the *real* structure of $Cu_2Mo_6S_8$ chevrel phase (CuCP) and its electrochemical behavior as a cathode material in novel, promising rechargeable Mg batteries. To obtain fast kinetics of Mg insertion into this material, its particle size was reduced to sub-micrometer scale by milling. We discovered an unusual instability of CuCP upon milling, which leads to a drastic decrease in the electrode capacity. The mechanism of this mechanical instability was investigated by XRD and XPS. The comparison of the CuCP mechanical stability with that of other chevrel phases (Ni, Sn, Pb, or Ag instead of Cu) reveals that the unusual behavior of CuCP is connected to the unstable oxidation state of the copper ions in this material. It was shown that milling of CuCP leads not only to an unusually deep amorphization of the material but also to a chemical reaction in which the Cu^+ ions are reduced and removed from the CuCP lattice.

Introduction

Chevrel phases, $M_xMo_6T_8$ (M = metal, T = S, Se, Te) were first discovered in the early 1970s, and since then there has been a lot of interest in these compounds because of their superconducting properties.[1–3]The unique crystal structure of these materials was well-established.[2–4] It was also shown that some chevrel phases could be used as cathodes for Li batteries.[5–7] Today, these compounds attract special attention as possible intercalation cathode materials for novel, promising rechargeable Mg batteries. In fact, at the moment, $M_xMo_6S_8$ chevrel phases are the only materials of the large family of intercalation compounds that are capable of inserting Mg^{2+} ions reversibly and in the wide range of x.[8] Moreover, the electrochemical characteristics of $Mg_2Mo_6S_8$ are suitable for practical battery design. However, chevrel phases as cathode materials have as yet hardly been studied, mainly because the field of rechargeable Mg batteries is still in its early development stage.

Two compositions seem to be the most attractive for Mg^{2+} intercalation/deintercalation: Mo_6S_8 and Mg_x-Mo_6S_8 (MgCP). The latter compound can be obtained by direct high-temperature (HT) synthesis (1000–1200 °C) from the elements or the sulfides.[1,3] However, first tests have revealed that MgCP obtained by direct HT synthesis possesses poor electrochemical activity, and the reason for this phenomenon is under study. Currently, the most promising material is pure chevrel framework, Mo_6S_8, free of any cation. Unfortunately, this compound is thermodynamically unstable and can be obtained only indirectly by chemical or electrochemical leaching of the more stable, cation-containing, chevrel phases, for example, $Cu_2Mo_6S_8$.[9,10] In our work, this composition was selected for its well-known synthesis and easy removal of Cu^+. In fact, leaching of $Cu_2Mo_6S_8$ under properly chosen conditions preserves the chevrel structure of this material.[9,10] As a result, all the peculiarities of the initial CuCP structure obtained by HT synthesis and the subsequent mechanical treatment should determine the electrochemical properties of the Mg batteries. Thus, it is important to study the correlation between the *real* structure of CuCP and its electrochemical behavior in magnesium ion containing electrolyte solutions.

It is well-known[11] that the electrochemical characteristics of intercalation compounds strongly depend on the morphology of the materials and on their structural perfection. For instance, a smaller particle size of the active materials usually facilitates faster kinetics of the electrochemical processes.[11,12] As a result, it is usually suggested that the particle size of the active mass of

(1) Chevrel, R.; Sergent, M.; Prigent, J. *J. Solid State Chem.* **1971,** *3,* 515.

(2) Yvon, K. In *Current Topics in Material Science*; Kaldis, E., Ed.; Elsevier, North-Holland, Amsterdam, 1979; Vol. 3, pp 53–129.

(3) *Superconductivity in Ternary Compounds I*; Fisher, Ø., Maple, M. B., Eds.; Springer: Berlin, 1982; p 221.

(4) Yvon, K.; Paoli, A.; Flukiger, R.; Chevrel, R. *Acta Crystallogr.* **1977,** *B33,* 3066.

(5) Schollhorn, R. *Angew. Chem., Int. Ed. Engl.* **1980,** *19,* 983.

(6) Coleman, S. T.; McKinnon, W. R.; Dahn, J. R. *Phys. Rev. B: Condens. Matter* **1984,** *29* (7), 4147.

(7) Tarascon, J. M.; Disalvo, F. J.; Murphy, D. W.; Hull, G. W.; Rietman, E. A.; Waszczak, J. V. *J. Solid State Chem.* **1984,** *54* (2), 204.

(8) Aurbach, D.; Lu, Z.; Schechter, A.; Gofer, Y.; Gizbar, H.; Turgeman, R.; Cohen, Y.; Moskovich, M.; Levi, E. *Nature* **2000,** *407,* 724.

(9) Chevrel, R.; Sergent, M.; Prigent, J. *Mater. Res. Bull.* **1974,** *9,* 1487.

(10) Schollhorn, R.; Kumpers, M.; Besenhard, J. O. *Mater. Res. Bull.* **1977,** *12,* 781.

(11) Winter, M.; Besenhard, J. O.; Spahr, M. E.; Novak, P. *Adv. Mater.* **1998,** *10,* 725.

(12) Weppner, W.; Huggins, R. A. *Annu. Rev. Mater. Sci.* **1978,** *8,* 269.

the insertion electrode be reduced as much as possible by grinding.[13,14] However, it was shown that in some cases[13,15,16] grinding leads to structural distortion of the materials and deterioration of their electrochemical properties.

The initial goal of this work was to study the influence of the mechanical treatment of CuCP on the performance of composite cathodes based on this material. However, in the course of the study, we discovered an unusual mechanical instability of the CuCP upon milling, which deserved special attention. It appears that application of mechanical forces on the CuCP induces remarkable solid-state reactions that were highly interesting to explore.

Experimental Section

The chevrel phases with the intended $Cu_2Mo_6S_8$, $Ni_2Mo_6S_8$, $SnMo_6S_8$, $AgMo_6S_8$, and $PbMo_6S_8$ composition were synthesized by reaction of the appropriate mixture of the powdered elements in an evacuated, sealed quartz tube. The procedure consisted of four sequential stages:

(1) Heating at 450 °C for 24 h.
(2) Heating at 700 °C for 24 h.
(3) Heating at 1050 °C for 48 h.
(4) Cooling down to room temperature at the rate of 120 °C/h.

Milling was performed in air using a Crescent-Wig L-Bug Amalgamator (Model 3110B). The powder (500 mg) of CuCP as well as a steel ball (6.35 mm in diameter) were put into a cylindrical stainless steel vial (2 cm³). The weight ratio between the steel ball and the chevrel powder was 2:1. In this grinding machine, the ball hits the powder particles, thus producing shock interactions.

The thermal treatment (annealing) of the milled material was performed in an evacuated, sealed quartz tube at 900 °C for 7 days to eliminate the structural distortion caused by milling.

The morphologies of the CuCP powders were studied by scanning electron microscopy (SEM) with JSM-6300 JEOL Inc. equipment (Japan).

The electrochemical behavior of CuCP electrodes was studied using a computerized Arbin Inc. (USA) multichannel battery tester. The electrode's active mass mixture (about 5 mg of CuCP + 10% carbon black + 10% PVdF) was applied onto a 1 × 1 cm² stainless steel foil. These electrodes, prepared after copper electrochemical leaching, were used as working electrodes in the cyclic voltammetry (CV) measurements. Electrochemical leaching of Cu^+ ions from CuCP was performed in 0.5 M $Mg(ClO_4)_2$/ACN solutions (galvanostatic mode, current 0.1 mA). CV (0.05 mV/s potential scan rate) was performed in a three-electrode cell. Solutions of 0.25 M Mg-$(AlCl_2BuEt)_2$ in THF (DCC/THF) were used as the electrolyte. Strips of Mg foil served as counter and reference electrodes.

XRD studies were performed with a Bruker Inc. (Germany) AXS D8 ADVANCE diffractometer (Cu Kα radiation). The surface chemistry of the CuCP powders was studied by XPS (Kratos Inc., England, Axis HS spectrometer).

Results and Discussion

SEM Morphology of Pristine and Milled CuCP. To obtain fast kinetics of Mg insertion into CuCP-based electrodes, the particle size of this material had to be

reduced to sub-micrometer scale. For this purpose, CuCP was synthesized and milled for different periods of time to vary the CuCP particle size distribution. Figure 1 shows SEM micrographs of pristine and milled CuCP. For the pristine material, it can be seen that sintering of small CuCP crystals upon HT synthesis resulted in the formation of relatively large, spherical agglomerates. The following micrographs show that the milling leads to deformation of the crystals' shape as well as to a loss of their initial integrity. This, in turn, forms new, large aggregates with a mechanical connection between the crushed crystals. As a result, by SEM inspection, we cannot observe drastic changes in the morphology of the CuCP crystals, for example, reduction of their particle size due to the milling.

Electrochemistry of Pristine and Milled CuCP: Drastic Loss of Capacity. The electrochemical behavior of the electrodes based on pristine and milled CuCP was studied by slow scan-rate cyclic voltammetry (SSCV). This method gives information about the specific capacity of the electrodes as well as some insights regarding the mechanism and the kinetics of the insertion/deinsertion processes. Figure 2 shows steady-state (0.05 mV/s) cyclic voltammograms of Mg insertion−deinsertion into composite electrodes based on pristine and milled (15 min) CuCP in a DCC/THF solution. The SSCV of the pristine material reflects a highly reversible process with a capacity above 100 mA·h/g. The most important feature that can be seen in Figure 2 is that the milled material possesses much less specific capacity than the pristine one, as can be calculated by integrating the SSCV curves (current vs time). Because of the drastic change in the specific capacity, it is impossible to compare the kinetics of the intercalation−deintercalation process in the two materials.

Figure 3 presents the results of similar experiments performed for the materials milled for various periods of time. The specific capacity of the Mg insertion−deinsertion into the Cu-leached chevrel phase is shown as a function of milling time. In this figure one can observe that the intercalation level attainable with the milled material is much lower than that of the unmilled material. It is important to note that these results were obtained with magnesium ions, which are known to be very sensitive to the crystallographic structure of the host material. Thus, the discovered critical phenomenon definitely warrants intensive investigation.

XRD Studies: Phase Transitions upon Milling and Annealing. To establish the reason for the discovered drastic loss in the capacity of the electrodes based on the milled CuCP, the *real* structure for the pristine and milled materials was compared by XRD analysis. Figure 4 shows the XRD pattern of the pristine CuCP (identical to the database CuCP−JCPDS-ICDD, 71-0215) and that of the material after 15 min and 1 h of milling. A drastic decrease of the diffraction peak intensity can be clearly seen. This decrease can only be explained by amorphization of the chevrel structure upon milling. Amorphization is a usual result of mechanical treatment. However, the mechanical instability of the material is remarkable.

To confirm the phenomenon of the unusual mechanical instability, several chevrel phases with different metal ions were synthesized, milled, and analyzed.

(13) Manev, V.; Momchilov, A.; Kozawa, A. *J. Prog. Batteries Battery Mater.* **1995**, *14*, 101.
(14) Disma, F.; Aymard, L.; Dupont, L.; Tarascon, J.-M. *J. Electrochem. Soc.* **1996**, *143*, 3959.
(15) Aladekomo, J. B.; Bragg, R. H. *Carbon* **1990**, *28*, 897.
(16) Cotton, F. A.; Wilkinson, G.; Murillo, C. A.; Bochmann, M. *Advanced Inorganic Chemistry*; John Wiley & Sons: New York, 1999; pp 855, 856.
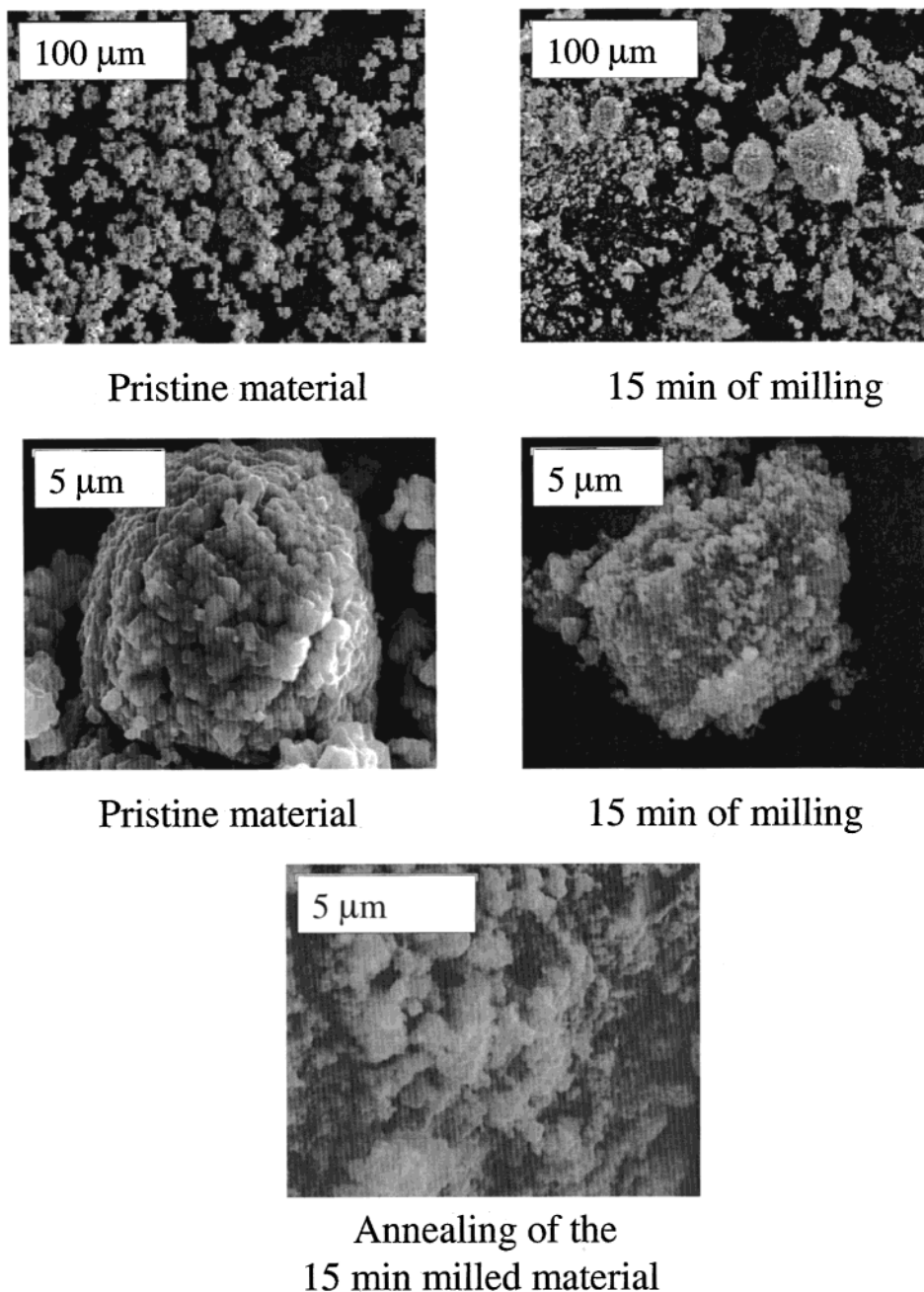
Figure 1. SEM micrographs of the pristine and milled CuCP at different magnifications.
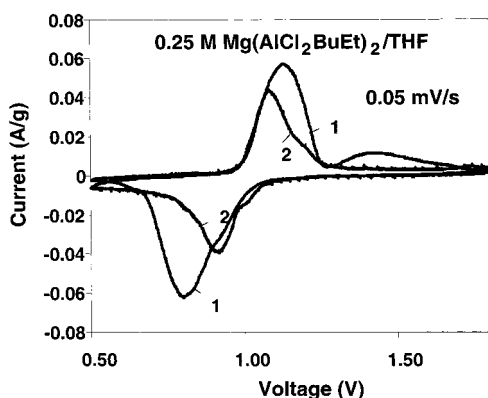

Figure 2. CV curves of the electrodes based on the pristine (1) and milled (15 min) CuCP (2).

Figure 5 shows the changes in the XRD patterns due to milling for a variety of chevrel phases (the reason for the phase selections will be discussed later): $Ni_2Mo_6S_8$ (identical to the database NiCP–JCPDS-ICDD, 78-1047), $SnMo_6S_8$ (identical to the database SnCP–JCPDS-ICDD, 25-0976), $PbMo_6S_8$ (identical to the database PbCP–JCPDS-ICDD, 33-0926), and $AgMo_6S_8$ (identical to the database AgCp–JCPDS-ICDD, 77-0494). As can be seen, none of these materials show evidence of an unusual mechanical instability as discovered for CuCP. Indeed, the XRD quantitative estimations of the remaining crystalline phases after 15 min of milling give ≈50% and 80% for CuCP and all other chevrel phases, respectively.

To investigate the mechanism of this phenomenon, a detailed XRD analysis of the pristine and milled CuCP was performed. The fine changes of the CuCP crystal structure associated with different durations of the mechanical treatment are presented in Figure 6. One can see the broadening of the diffraction peaks and the
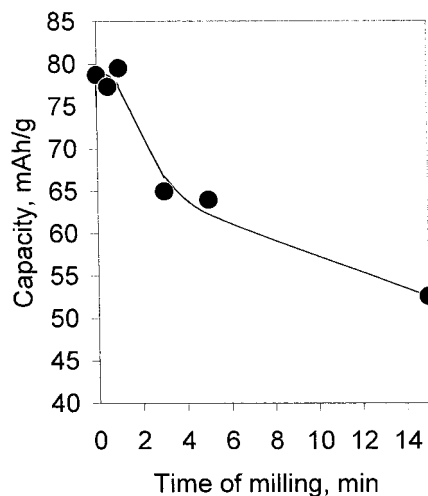
Figure 3. Dependence of the specific capacity of CP electrodes in electrochemical Mg insertion on the CuCP milling time.
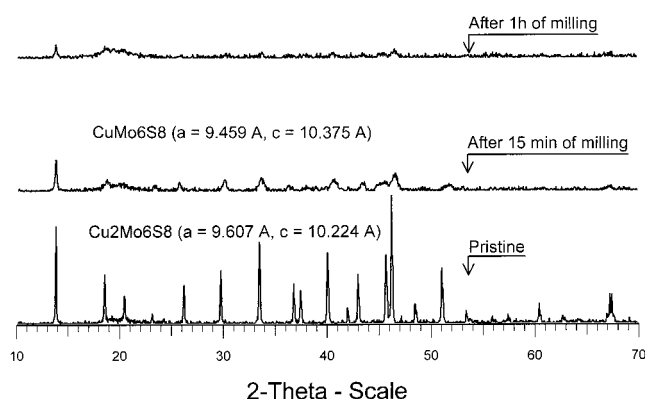

Figure 4. XRD patterns of the pristine and milled CuCP.

decrease in their intensities with an increase in the milling time. These changes are typical for milling processes. They are connected with a decrease of the crystallite sizes, increase in the crystal structure distortions, and material amorphization. Surprisingly, a careful check of the diffraction patterns after milling reveals not only the above specific features but also a shift of the diffraction peaks from the initial positions. This shift cannot be related to peak superposition, but to significant changes in the unit cell parameters upon milling. The latter are indicative of changes in the chemical composition of the CuCP upon milling. This result is also very unusual. It is not expected that mechanical treatment will cause changes in the chemical composition of the milled material.

How can we determine the chemical composition of CuCP? Figure 7 shows the dependence of the unit cell parameters on the Cu^+ content in CuCP. These graphs were drawn according to the data in ref 4 for well-defined synthesis products with various stoichiometries. (The accuracy of the unit cell parameter determination was 0.002 Å.) Using this dependency, the stoichiometry of CuCP can be determined accurately on the basis of the values of the unit cell parameters. These parameters as well as the compositions corresponding to them are presented in Figure 8 for the pristine CuCP and for the material after 15 min of milling. (The accuracy of the unit cell parameter determination was 0.005 Å.) Thus, the Cu^+ content, calculated according to the unit cell
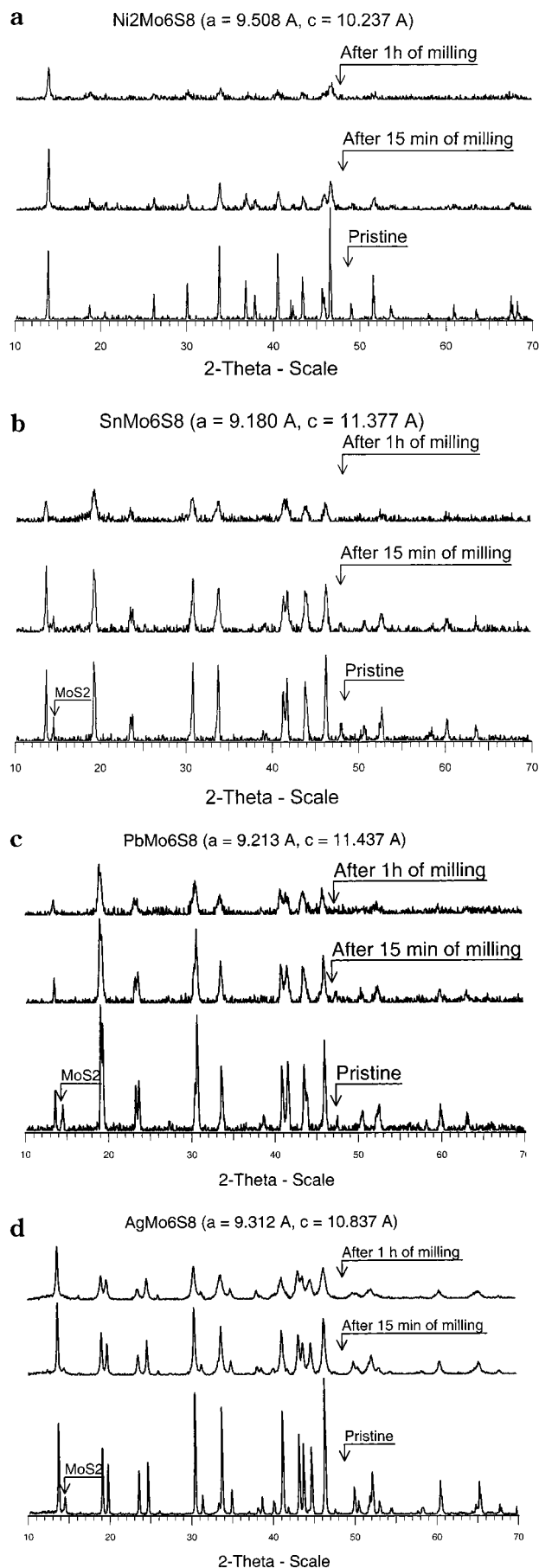

Figure 5. XRD patterns of the pristine and milled chevrel phases with the intended composition: (a) $Ni_2Mo_6S_8$, (b) $SnMo_6S_8$, (c) $PbMo_6S_8$, and (d) $AgMo_6S_8$.
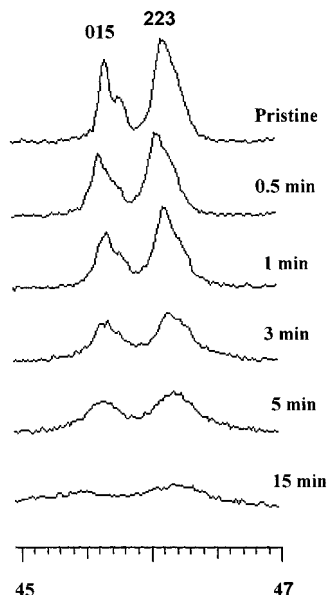
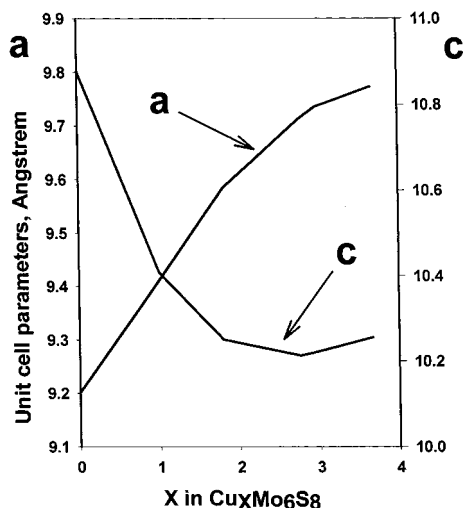**Figure 6.** Detailed XRD patterns of the pristine and milled CuCP.

Figure 7. Variations of the unit cell parameters on the Cu^+ content in CuCP.

parameters for $Cu_xMo_6S_8$ after 15 min of milling, changes from $x = 2$ to $x = 1$.

As has been shown, XRD analysis allows the estimation not only of the amount of the crystalline phase after milling but also of the chemical composition of this phase. However, the obtained data are not sufficient for understanding all the effects that take place upon milling. For instance, XRD data described earlier do not give compositional information about the amorphous part of the milled materials. Unfortunately, the amorphization limits the usability of the XRD method. Nevertheless, phase analysis for amorphous materials by XRD is possible. For such analysis, a heat treatment that converts the material to a crystalline phase has to be done. Moreover, in the current case, the annealing of the milled material may be useful for studying the capability of the amorphous part to return to its initial crystal structure.

Figure 8 shows the XRD patterns of the milled material (15 min of milling) before and after annealing. First of all, we can see the increase in the intensity of
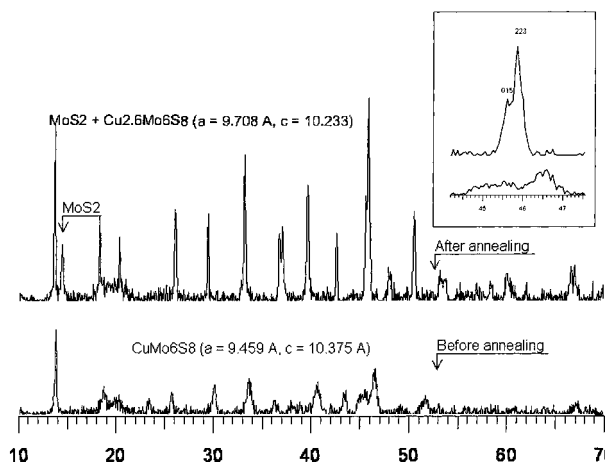

Figure 8. XRD patterns of the milled material (15 min of milling) before and after annealing.

the diffraction peaks and the drastic decrease in their width. This is a typical change that is connected to the perfection of the crystal structure upon annealing. The reconstruction of the initial crystal shape can also be seen on the SEM micrograph for the annealed CuCP (Figure 1). Besides that, unusual evolution can be noted by comparing these two XRD patterns: the appearance of a new crystalline phase, MoS_2 (identical to the database MoS_2—JCPDS-ICDD, 37-1492, with a characteristic diffraction peak at $2\theta = 14.5°$) and the shift of the diffraction peaks of the CuCP due to the change in the unit cell parameters. These parameters are also shown in Figure 8. According to the graph in Figure 7, these parameter changes correspond to the change of the $Cu_xMo_6S_8$ composition from $x = 1$ to $x = 2.6$. Hence, the amorphous phase, obtained upon milling, transforms during annealing to the crystalline and thermodynamically stables material MoS_2, while copper reinserts into the structure of the CuCP. However, the amount of CuCP after milling and subsequent annealing is less than that in the initial material. (As has been mentioned, the XRD analysis of the annealed material shows a mixture of MoS_2 and CuCP). As a result, the Cu^+ content in $Cu_xMo_6S_8$ rises.

A scheme of the phase transitions occurring upon milling and annealing is presented in Figure 9. This scheme is based on the analysis of the XRD data.

XPS Study: Changes in the Oxidation State of the Cu. As has been shown by XRD analysis, the mechanical instability is associated with phase transitions and Cu ion migration. However, XRD analysis taught us nothing about the nature of the copper in the amorphous part of the milled material. It has been assumed[2] that Cu ions in CuCP are monovalent. However, the oxidation state of Cu ions might change during their migration upon milling. An XPS analysis of the pristine and milled CuCP materials was performed to learn about possible changes in the oxidation state of copper. Figure 10 presents the results of the XPS analysis in the Cu $2p^{3/2}$ emission region for pristine chevrel and the materials after 0.5 and 15 min of milling. For pristine chevrel, a large peak centered at 934.5 eV can be attributed to Cu^+, with a small shoulder on the lower binding energy side that is probably due to Cu with a metallic character. For the milled materials, the latter shoulder grows into an intense peak
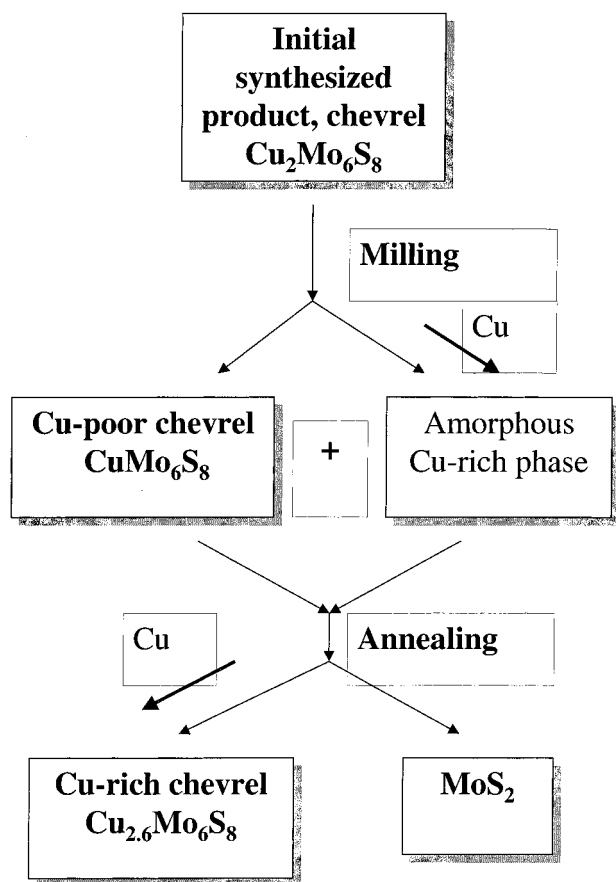
Figure 9. A scheme of the phase transitions occurring upon milling and annealing.

Figure 10. Cu 2p XPS spectra for a pristine CuCP and the same materials after 0.5 and 15 min of milling.

centered at 932.6 eV that can be associated with metallic Cu. The ratio of the peak intensities for Cu^+ and metallic Cu increases with milling duration. Thus, a combination of the XPS and the XRD analyses reveals that the unusual instability of CuCP upon milling is associated with the partial removal of Cu^+ ions from the chevrel structure and their transformation to metallic copper.

Possible Reasons for the Unusual Mechanical Instability. The XRD analysis reveals an unusual mechanical instability of CuCP. For a comparison, graphite, which is bound by weak van der Waals bonds between the graphene layers, retains its crystalline structure even after 20 h of milling under similar conditions.[14] Contrary to graphite, there are no weak chemical bonds in the crystal structure of chevrel (Figure 11). Indeed, there are metallic bonds between the Mo atoms that build the octahedral clusters, covalent bonds between Mo and S atoms, and ionic bonds between S and Cu atoms. The latter bonds seem to be the weakest ones. Thus, it is reasonable to suggest that the destruction of the material is associated with the breaking of these ionic bonds.

The strength of ionic bonds between two adjacent atoms can be easily estimated using the following equation,

$$F = cq_1 q_2 e^2 / r^2$$

where q_1 and q_2 are the oxidation states of these atoms, e is the electron charge, r is the distance between these atoms, and c is the constant for the appropriate units.
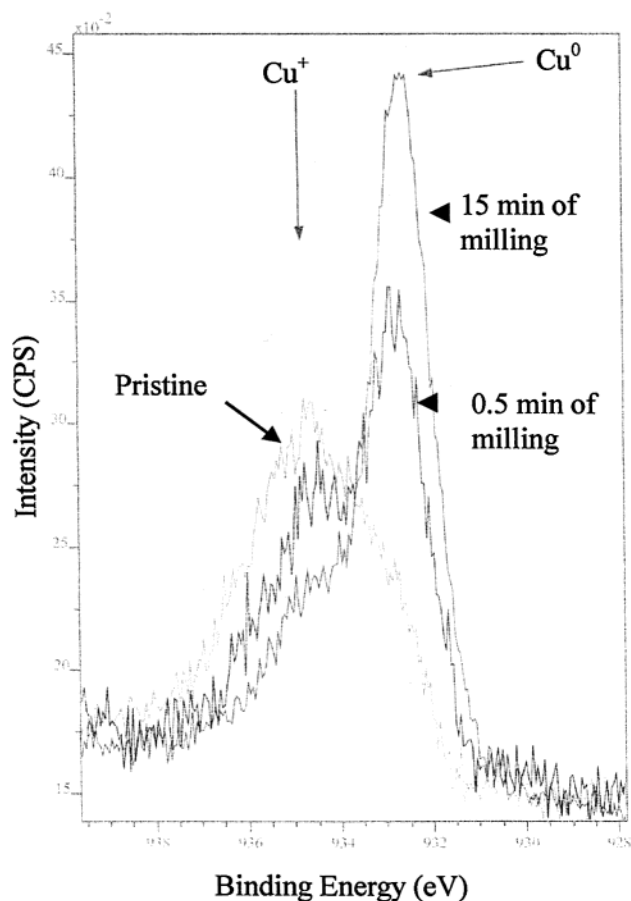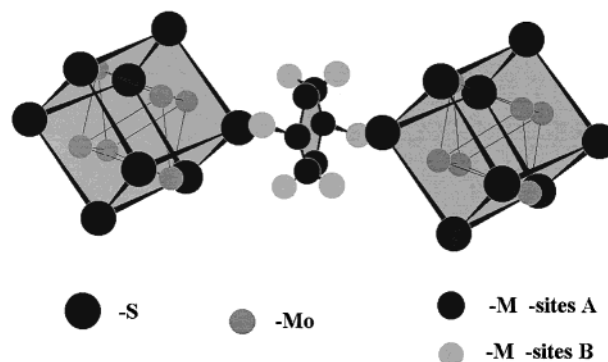

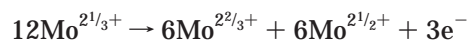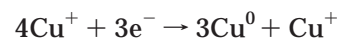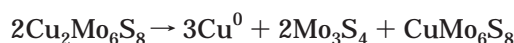**Figure 11.** The crystal structure of chevrel.

A simple estimation, based on the equation above, provides a value for CuCP that is only 4 times lower than that of the $LiMn_2O_4$ spinel, a commonly used cathode material for rechargeable Li batteries and which is known to be mechanically robust. Thus, this estimation seems to indicate that the mechanical instability of CuCP is really unusual and it could not be understood just in light of electric forces of the ionic bonds in this material.

The results of the XRD revealed that the unusually deep amorphization of CuCP is associated with Cu ion migration. The question arises as to whether the effect of the mechanical instability is a unique feature of CuCP or whether this effect results from the unusual crystal structure that ensures the high mobility of the metal ions for some chevrel phases? What do we know about

the cation's positions in the crystal structure of chevrel and their mobility? It is known[2,3] that the occupation of the different crystallographic positions in the crystal structure of chevrel depends on the size of the metal ions: large cations such as Pb^{2+} or Sn^{2+} occupy the position in the center of the cube formed by the sulfur ions (special crystallographic position), while small cations such as Cu^+ or Ni^{2+} can partially occupy the tetrahedral positions connected to a ring (general crystallographic positions). It should be noted that only the places which can be occupied by small cations are shown in Figure 11. The position of the large cations is in the center of the ring shown in Figure 11. The large cation distribution on the special crystallographic positions causes immobility of these cations that can be demonstrated by electrochemical means or by conductivity measurements.[2,3] The small cation distribution on general crystallographic positions leads to high cation mobility, which is responsible for the high ionic conductivity of the relevant chevrel phases and their easy electrochemical leaching.

To clarify the role of cation mobility, the mechanical stability of a variety of chevrel phases with the $Ni_2Mo_6S_8$ (another case of a small cation with high mobility), $SnMo_6S_8$, $PbMo_6S_8$, and $AgMo_6S_8$ (three cases of large, immobile cations) compositions were studied. Note that the oxidation state of the Ag^+ cation in the last compound is the same as that of CuCP. As has been shown by XRD analysis, none of these materials show evidence of an unusual mechanical instability as discovered for CuCP. Thus, the unusual mechanical instability is a unique feature of CuCP and cannot be explained by high mobility of the Cu ions in the crystal structure of chevrel.

It is well-known[16] that many Cu^+ ion compounds are not stable. Some of them, like CuI, are easily oxidized by air oxygen. In this case, Cu^+ transforms to the more stable Cu^{2+}. Thus, it is reasonable to assume that the mechanical instability of CuCP might be connected with the chemical instability of the monovalent Cu^+ ions. In fact, on the basis of XRD and XPS data, we can suggest that the unusual mechanical instability of CuCP is connected to a chemical reaction induced by the milling process. This reaction seems to be written as

$$2Cu_2Mo_6S_8 \rightarrow 3Cu^0 + 2Mo_3S_4 + CuMo_6S_8$$

$$4Cu^+ + 3e^- \rightarrow 3Cu^0 + Cu^+$$

$$12Mo^{2^1/_3+} \rightarrow 6Mo^{2^2/_3+} + 6Mo^{2^1/_2+} + 3e^-$$

Here, the valence of the Mo ions are $+2^1/_3$ in $Cu_2Mo_6S_8$, $+2^2/_3$ in Mo_3S_4, and about $+2^1/_2$ in $Cu_{2-x}Mo_6S_8$ in the event that $x \approx 1$ (15 min of the milling). Thus, in contrast to the oxidation of copper, as is usual for many Cu^+ compounds, reduction of Cu^+ to metallic copper takes place in this case. The possible reason for this is the more preferable oxidation of Mo ions during the conversion of the chevrel phase to the more stable, layered MoS_2.

As has been mentioned, the chemical reaction induced by mechanical treatment leads to the changes in the chemical composition of CuCP as well as to unusually deep amorphization of the material. This amorphization results in a dramatic decrease of the electrochemical capacity of the electrodes based on the milled CuCP.

Conclusions

The combination of the XRD and XPS methods were used to explore the mechanism of the unusual mechanical instability of the CuCP, a material used as the active mass in cathodes for new rechargeable Mg batteries. It was shown that milling results not only in the unusually deep amorphization of the initial crystal structure but also in the partial removal of Cu^+ ions from CuCP and their transformation to metallic copper. The comparison between CuCP and chevrel phases with different cation compositions revealed that the effect of the mechanical instability is connected to the unstable oxidation state of the copper ions rather than to a peculiarity of the CuCP crystal structure, such as the high mobility of Cu^+ ions. Thus, the mechanical treatment provides a chemical reaction associated with Cu^+ ion reduction/Mo ion oxidation. The partial amorphization of the initial CuCP crystal structure upon milling results in the drastic decrease of the electrochemical capacity of the electrodes based on this material.